

13. DOPPLER-FREE SPECTROSCOPY

James C. Bergquist

National Institute of Standards and Technology
Boulder, Colorado

13.1 Introduction

Spectroscopy is an important tool for investigating the structure of physical systems such as atoms or molecules. Thermal motion of free atoms and molecules gives rise to Doppler broadening of the characteristic spectral transitions, which often blurs important details of the spectra and prevents a deeper understanding of the underlying physics. Long before the appearance of lasers, well before their use in nonlinear, high-resolution spectroscopy, long before laser-cooling, atomic and molecular beams had been used for high-resolution spectroscopy. And, perhaps not surprisingly, beam techniques remain prominent in spectral studies. In the course of this chapter, we will seek a rudimentary appreciation of the methods used to reveal Doppler-free spectra. But first we will begin with a brief discussion of motional effects that produce line broadening and shift, before we address their countermeasures.

13.2 Spectral Line-Broadening Mechanisms

Atoms or molecules in gases can be relatively free and undisturbed, but their spectral lines are spread out over a range of frequencies by the Doppler effect because they are moving in all directions with high thermal velocities. Those particles moving toward an observer absorb light at lower frequencies than those at rest; those receding absorb at higher frequencies. The resulting Doppler broadening can often mask spectral fine and hyperfine structure, even though each individual absorber still retains its typically much narrower natural line width. The spectral line of a moving particle is shifted away from its rest-frame frequency ω_0 to $\omega_0 + \mathbf{k} \cdot \mathbf{v}$, where \mathbf{k} is the wave vector of the interrogating radiation and \mathbf{v} is the velocity of the particle. Since the particles move isotropically in all directions, the Doppler shift is different for each particle; this is an example of inhomogeneous broadening. At thermal equilibrium the velocity distribution is Maxwellian:

$$w(v) = \left(\frac{1}{\sqrt{\pi}u} \right) \exp(-v^2/u^2), \quad u = (2k_B T/m)^{1/2}, \quad (13.1)$$

where m is the particle's mass, T is the temperature (in kelvins), and k_B is Boltzmann's constant. The spectral lineshape of the ensemble is obtained by the convolution of the lineshape of an individual particle with a Maxwellian distribution of velocity-projected frequency shifts. The result is the Voigt profile with a characteristic spectral width at half maximum (FWHM) given by

$$\Delta\omega_D = (2\omega_0/c)((2kT/m) \ln 2)^{1/2}. \quad (13.2)$$

For quantum absorbers with an atomic mass near 100 uu and near room temperature (300 K), the Doppler width $\Delta\omega_D \sim 10^{-6}\omega_0$. For optical frequencies $\omega_0 \sim 2\pi(5 \times 10^{14} \text{ Hz})$, Doppler broadening ranges from 10^8 to 10^{10} Hz. Laser-cooling routinely produces atomic temperatures below 10^{-3} K, but the Doppler width even at 1 μK remains substantial, ranging from 10^4 to 10^6 Hz. For high-resolution spectroscopy of ultracold free particles, Doppler-free interrogation is still important.

The motion of atoms or molecules broadens and shifts spectral features through other mechanisms as well. The finite interaction time of the particles with the radiation field produces line broadening due to the energy–time uncertainty principle. We may solve for the lineshape as the Fourier time transform of an undamped harmonic oscillator viewed for a finite time interval Δt . The magnitude of the FWHM is

$$\Delta\omega_t \approx 2\pi(0.89)/\Delta t. \quad (13.3)$$

This broadening effect very often results from the travel time $\Delta t = L/v$ of a freely moving quantum system through a radiation region of finite extent L . If the radiation field is not uniform, but rather is a nearly planar Gaussian beam that probes the atoms perpendicular to their velocity, then the spectral lineshape has a linewidth

$$\Delta\omega_t = (2\sqrt{2} \ln 2)(v/w_0), \quad (13.4)$$

where $2w_0$ is the Gaussian beam diameter. This spectral width is nearly the same as that obtained for the finite uniform light field with $L = 2w_0$. The wave surface of a Gaussian beam is strictly not planar, but curved away from its beam waist. The curvature of the wave surface through which the atom passes restricts the effective transit time and broadens the line. The line width is [1]

$$\Delta\omega_R = (2v\sqrt{2} \ln 2)(w_0^{-2} + w_R^{-2})^{1/2}, \quad (13.5)$$

where $w_R = R\lambda/\pi w_0$, and R is the radius of curvature of the Gaussian light beam. In order that the curvature of the probe field not significantly broaden the line above the transit time limit, $R \gg \pi w_0^2/\lambda$. For thermal velocities near $T = 300$ K, transit time linewidths typically vary from 10^3 to 10^5 Hz.

above the transit time limit, $R \gg \pi w_0^2/\lambda$. For thermal velocities near $T = 300$ K, transit time linewidths typically vary from 10^3 to 10^5 Hz.

Another pernicious effect of atomic motion is the spectral line broadening caused by interparticle collisions or collisions with the walls of the vessel that confines the gas. Such collisions intermittently alter the phase of the resonance frequency of the particle and sometimes cause the cessation of the atomic precession (state decay). State decay can occur in a collision if the energy difference between atomic levels is not large compared to the kinetic energy of the collision partners. Hence, collisions causing state decay are relatively rare in the case of optical transitions in atoms, but are not uncommon for mid-infrared transitions in molecules. Usually, collisions that cause state decay are treated phenomenologically as a modification to the natural decay rate, so the spectral line is broadened, but not shifted. The amplitude of the atomic phase change caused by a random collision depends on the relative impact parameter and velocity of the colliding partners. If the phase change $\Delta\theta \ll \pi$, then the spectral feature is not broadened, but it is shifted by the average phase shift $\langle\theta\rangle$ to $\omega_0 + \langle\theta\rangle/\Delta t_c$ where t_c is the mean duration time between collisions. For stronger collisions, $\Delta\theta \gg \pi$, and the phase of the atomic oscillation is abruptly changed during the short collision time. The atomic resonance is not shifted in this process, but it is broadened to [1]

$$\Delta\omega_c \approx 2/\Delta t_c. \quad (13.6)$$

The interparticle broadening due to collisions is pressure dependent with typical molecular values that range from 8 to 240 kHz/Pa (1–30 MHz/torr). If the pressure is reduced until the mean free path exceeds the dimensions of the gas cell, then wall collisions dominate. Particles that collide with the cell wall can also state-decay, but most certainly suffer velocity changes and phase shifts that generally terminate their contribution to the signal. The line broadening is inversely proportional to the transit time of the particle across the cell. However, in the next section we will show that, in some cases, collisions can lead to Doppler narrowing!

13.3 Spectral Line-Narrowing Techniques

Limitations in optical spectroscopy caused by the broadening and shift due to thermal motion have been reduced and even eliminated by numerous techniques developed over the past half-century. The first generally productive countermeasure to Doppler broadening was the method of atomic beams developed in the 1930s and still widely used [2]. The idea is straightforward: $\mathbf{k} \cdot \mathbf{v}$ is minimized by probing *all* atoms in a direction that is nearly perpendicular to the atomic motion. The direction of the velocity vector is restricted to a small cone by a collimator (or a sequence of collimators) placed in front of an effusive source.

The particles travel out from the source through the collimator into a high-vacuum region, where they are intercepted by the probe radiation. The practical degree of collimation ranges from 10 to 10^3 , which reduces the Doppler broadening proportionally. For oven temperatures near 300 K or higher, Doppler widths of atomic beams remain stubbornly large ($\geq 10^7$ Hz). Higher collimation is possible but lowers the particle flux and thereby the signal. The loss in signal-to-noise ratio is tolerable if substructure can be revealed. Laser-cooling of the atomic source makes possible intense beams of cold atoms (even near monovelocity beams of atoms). Cold atomic beams are discussed elsewhere in this volume, but as stated earlier, temperatures near 10^6 K still give Doppler broadening near 10^3 – 10^5 Hz for atomic transitions in the visible.

The high intensity per unit bandwidth characteristic of lasers makes it possible to virtually eliminate the first-order Doppler broadening in gas samples. This can be done with either of two nonlinear techniques, saturated absorption [1, 3–6] or two-photon spectroscopy [1, 3, 4, 8, 9]. In saturation spectroscopy, a group of absorbers in a narrow interval of axial velocities is labeled by their nonlinear interaction with a monochromatic traveling laser wave, and a Doppler-free spectrum of these velocity-selected absorbers can then be observed with a second laser beam used as a probe. In order to be sensitive to the natural resonant frequency in the laboratory frame, parallel, counter-running waves of the same frequency (which may or may not be coincident spatially) are used. Since the Doppler shifts have the opposite sign for the two beams, the two traveling-wave frequencies are viewed as equivalent only by absorbers essentially free of velocity along the light axis. Thus, if the laser is tuned to the absorber's resonant frequency, the two waves work together to saturate the same "zero velocity" class of absorbers, which then produces a narrow spectral resonant feature [5–7].

In two-photon spectroscopy, the transition energy of the atom or molecule is provided by the simultaneous absorption of two photons. If the photons each are absorbed from one of two counter-traveling waves that have the same optical frequency, then the Doppler shift $\mathbf{k} \cdot \mathbf{v}$ of one photon is precisely cancelled by the Doppler shift of the other photon. The condition for resonance is that twice the field frequency equals the unshifted frequency of the two-quantum transition. Independent of their velocities (ignoring second-order Doppler effects), all atoms contribute to the two-photon Doppler-free signal at $\omega = \omega_0$. This is in contrast to saturation spectroscopy, where only a small slice of the velocity distribution that is essentially normal to the laser beam can interact with the radiative driving field. Two-photon spectroscopy has other advantages compared to saturated absorption spectroscopy [1, 3, 4].

The resonance is not broadened or shifted by wavefront curvature of the light beams (*provided* that the wavefronts of the counter-running beams are matched), because the two photons are absorbed simultaneously. In saturated absorption

studies, the wavefronts needed to be flat in order to well define the narrow velocity distribution needed for high resolution. Since the direction of atomic motion is not important in two-photon spectroscopy, long interaction times are made possible by using an atomic beam directed along (or at a small angle to) the optical axis. In saturation spectroscopy, the atomic motion must be orthogonal to the light beam; for long interaction times, large-aperture optics of high quality (expensive) are needed to give a resolving power limited by transit-time broadening. Two-photon spectroscopy is not without its problems. Residual first-order Doppler effects will remain unless the wavefronts of the counter-running beams are perfectly matched, that is, the wavevectors must be oppositely directed everywhere. Wavevectors can be arbitrarily well opposed by carefully mode-matching the laser beam into an optical cavity that also serves to enhance the intensity in the light beams. A relatively large broadening and shift are produced by the optical Stark effect. In the general case, the coefficients for the optical Stark shift and for the probability for the two-photon transition are nearly the same. Therefore, a compromise must be struck between signal strength and Stark shift.

In Section 13.2, we remarked that particle collisions change the velocity of the quantum radiators interacting with the light field, which can *reduce* Doppler broadening. This narrowing can result if the particle's motion is altered, but otherwise there is little or no change in the phase of the oscillator during the collision. In other words, it is important that the precession frequencies of the particles remain phase-coherent (or nearly so). If there are many collisions during the effective decay time of the particle's oscillation, then the Doppler-shifted frequency $\omega_0 + \mathbf{k} \cdot \mathbf{v}$ is frequently altered and essentially averaged to zero. This is termed Dicke narrowing after the author who first described it [10]. Significant narrowing occurs if the collisions confine the particles to volumes with dimensions smaller than the wavelength of the interrogating light and the decay rate of the oscillating dipole remains small ($\gamma \ll 1/\Delta t_c$). Until recently, this has been difficult at optical frequencies, where collisional broadening simply overwhelms any Dicke narrowing. However, laser-cooling and trapping of atoms [11] and ions [12] have revived interest in Dicke's method applied to Doppler-free spectroscopy; we will give an example and a more complete discussion of Dicke narrowing in the last section of this chapter.

Armed with these and other Doppler-free techniques, spectroscopists have pushed fractional resolution in the optical domain to nearly 1×10^{-15} . Pressure broadening and shift and geometrical broadening and shift offer a practical challenge, but in many experiments, these have been virtually eliminated. The spectral width of naturally narrow optical transitions is most often dominated by transit-time broadening and second-order Doppler effects (*and* by the spectral purity of the laser, but that is a topic to be treated in the third volume of this series, *Electromagnetic Radiation*). Second-order Doppler effects can be

partially reduced by labeling and using one velocity class of absorbers, but only with a loss in signal. Clearly, most broadening and shift problems would be reduced if the particle temperature were lowered. Particles at rest have no motional effects. It is understandable, then, that laser-cooling of free and trapped particles has become a prominent tool in the research and spectral studies of many atomic physicists.

For room-temperature gas samples, one quickly encounters practical limits (and in the case of saturated absorption, loss of signal) when the interaction time is increased. A partial circumvention of the practical limitations imposed by transit-time broadening uses the interference that arises from the sequential interactions of the induced dipole of a quantum absorber with radiation fields separated in time [13–15]. Transit-time broadening is then determined by the temporal separation of the light fields. In our first example, we will look more closely at the Ramsey method of separated atom–field interaction regions and why it is particularly useful in saturated absorption.

13.4 Saturated Absorption with Ramsey Interference Fringes

With the elimination of first-order Doppler effects, attention turned to the resolution limitation imposed by interaction-time broadening. To be transit-time limited in saturated absorption spectroscopy, the projection of atomic motion onto the radiation-field axis must be such that $\mathbf{v} \cdot \mathbf{k}$ is less than the inverse of the transit time through the beam. Hence, the greater the resolution, the stricter the velocity selection, and so fewer atoms contribute to the signal. A particularly simple yet powerful scheme to greatly reduce interaction-time broadening and attain spectrally narrow lines at microwave frequencies was proposed by Ramsey [13]. He suggested intercepting a beam of atoms with spatially separated radiation fields (derived from the same source) so that independent phase evolution of atoms and radiation field could occur during the free flight of the atoms between fields. Temporal modulation of the field could also be achieved by pulsing the field on and off, provided that the atoms were slow enough to remain in the interaction region or were otherwise confined spatially. The interaction of absorber and field in the first radiation beam (pulse) produces a coherent superposition of upper and lower states. The induced atomic polarization precesses at the natural resonance frequency in the field-free region between the radiation zones (between pulses). The effect of the second light field (pulse) on the atomic transition probability depends on the relative phase of the radiation field to the absorber's oscillation, so the absorbers passing through the second field (pulse) will either be further excited or returned to the ground state. Thus, an interference results, because the quantum absorption transition probability no longer depends only on the frequency of the driving field, but also on the

phase-evolution difference of the atom and the field during the free flight of the atom between zones (between pulses). The phase difference is proportional to the product of the frequency detuning of the radiation field from resonance ($\omega_0 - \omega$) and the interzone (interpulse) transit time T . For spatially separated beams, $T = L/v_x$, where L is the interzone spacing and v_x is the atomic speed orthogonal to the axis \mathbf{z} of the light beams and in the plane containing them. In the pulsed case, the free precession period is independent of the atomic velocity. Note that on resonance, all atoms constructively contribute to the signal independent of their velocities (ignoring, for the moment, second-order Doppler effects). The central fringe of the Ramsey absorption profile is centered at $\omega = \omega_0$, with a spectral width determined by the time between the radiation regions (pulses), rather than by the transit time through each region (pulse time). However, synthesis of Ramsey's idea and saturated absorption in the optical domain is difficult because the wavelength is shorter than the dimensions of the interaction region. Even in a well-collimated atomic beam, there will be a spread of the residual Doppler velocity projections v_z on the direction of light wave propagation. Likewise, in saturated absorption spectroscopy, the criterion that $\mathbf{v} \cdot \mathbf{k}$ be less than the inverse of the interaction time in the first light beam (pulse) does not prevent a spread of the atoms over several wavelengths in the second light beam.

By way of example, consider a beam of quantum absorbers crossing a collimated laser beam of waist size w_0 . Near perpendicular incidence, there is a narrow acceptance angle, $\delta\theta \equiv v_z/v_x \approx \lambda/\pi w_0$, in which the accumulated phase difference between the field frequency and the Doppler-shifted frequency (seen by the moving absorber) never exceeds π radians. That is, absorbers within this slice enter and leave the radiation field before any mismatch of their frequency to the field frequency is recognized (transit-time broadening exceeds the residual Doppler broadening). Adding a second optical interaction zone a distance L downstream does not lead to strong Ramsey fringes because the angular slice defined by the first interaction maps into a large extension, $\Delta z = L \cdot \delta\theta = L\lambda/3w_0$, in the second field interaction region. The condition for increased resolution by the Ramsey interference, $L/w_0 \gg 1$, is just the condition that the dipoles originating at one spatial position in the first light field will be spread out over several wavelengths in the second field region. The Ramsey signal is spatially averaged to zero, since particles with the *same* field-free precession time experience *different* phases of the second driving field dependent on their spatial entry position into the second zone. The same arguments apply to the pulse interrogation method.

Baklanov and his colleagues introduced the idea of a third, equally spaced interaction zone as a method to recover the Ramsey fringes [14]. However, as a way to better see the phase relationships leading to the interference signal, it is more convenient to assume four interaction zones (pulses) [15–17]. In saturation

spectroscopy, the narrow resonances arise from four conceptually separate time-ordered interaction processes: lower state population to dipole, dipole to upper state population, upper state population to dipole, and finally, dipole dotted with the field to project out the excitation probability. The saturated absorption Ramsey interference signal develops when the interactions occur sequentially, one per zone (pulse). As in the RF and microwave case, the dipole prepared by the first interaction will precess at its own natural frequency ω_0 and decay with a dipole decay rate γ_{ab} in the darkness between the first two light beams (pulses). In the second interzone (interpulse) space, the excited-state population will only decay, with the population decay rate γ_b . In the third interzone (interpulse) space, the system again carries a dipole moment and precesses and decays as before. Assuming the interzone (interpulse) times to be T , aT , bT , respectively and ignoring the field phase (assumed fixed) leads to the expression for the total phase of the Ramsey signal [15]:

$$\begin{aligned} \exp[i\phi_{\text{total}}] = & \exp[-ikv_z(b-1)T] \exp[-i(\omega - \omega_0)(b+1)T] \\ & \times \exp[-\gamma_{ab}(b+1)T] \exp[-\gamma_b aT]. \end{aligned} \quad (13.7)$$

Because of the distribution of v_z values, the Ramsey fringes appear only for the case $b = 1$, that is, when the dipole free precession times are equal. The second field-free region does not improve spectral resolution, but it can enhance the Ramsey signal [16, 17]. We can also show that the fringes arise only for the case of two separated interactions with parallel, co-running beams followed by two separated interactions with parallel, oppositely running beams. The spatial modulation in the atomic response produced by the first two field interactions can be exactly unfolded in the probe process to reveal the narrow Ramsey signal, but only if the second two interactions are separated by the same time interval as the first two. Unfolding the spatial modulation to reveal the narrow Ramsey structure has two important consequences:

- Essentially all atoms for which the broadening due to the field interaction time exceeds the residual Doppler broadening contribute to the Ramsey interference signal. If the radiation field filled the entire effective aperture $2L$ (or if the pulse duration extended for the effective free precession time $2T$), then only those absorbers with $v_z \leq \lambda v_x / 2\pi L$ ($v_z \leq \lambda / 2\pi T$) would contribute to the signal. Thus, the Ramsey method permits significant line narrowing with essentially no loss in signal. In fact, it is best to shorten the field interaction time to increase the number of contributing atoms.
- Large aperture optics are not necessary.

Saturated absorption optical Ramsey fringes were first observed in the experiment shown in Figure 1 [15], where a fast ($v/c \approx 10^{-3}$), monovelocity ($\Delta v/v \approx 10^{-4}$) beam of metastable ^{20}Ne atoms sequentially interacted with spatially separated light beams from a frequency-stabilized dye laser. The

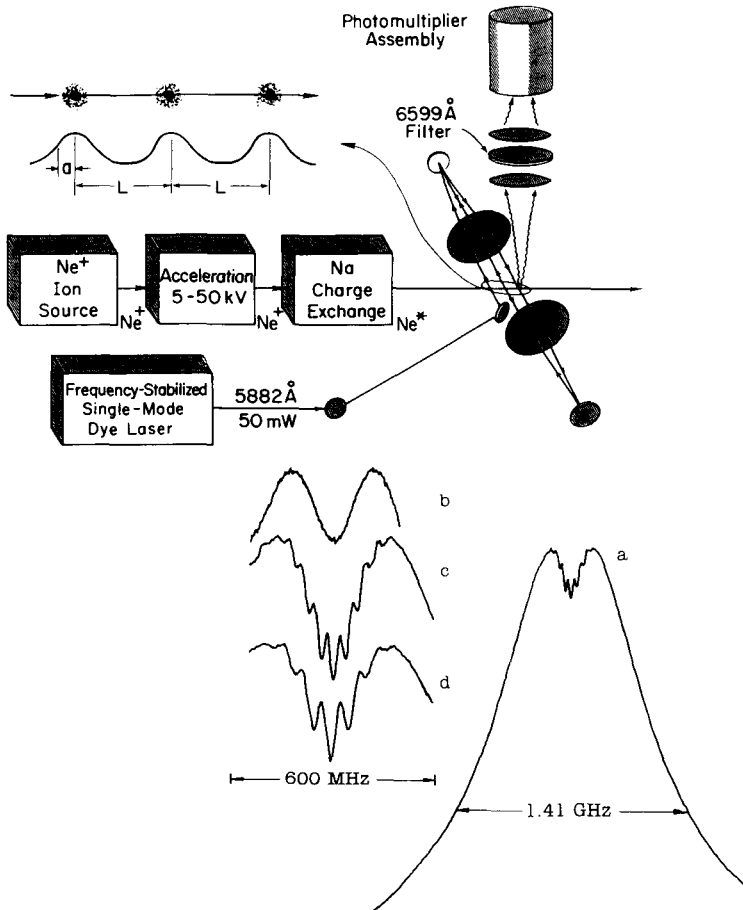


FIG. 1. Optical Ramsey fringes. The experimental setup is shown at the top of the figure. A fast ($v/c \sim 10^{-3}$) monovelocitory ($\Delta v/v \sim 10^{-4}$) beam of metastable neon atoms sequentially interacts with three spatially separated, standing-wave light beams formed by the opposition of two cat's-eye retroreflectors. A dye laser at 588 nm drives the $1s_5-2p_2$ transition and the excitation probability is monitored by fluorescence emission on the $2p_2-1s_2$ transition at 660 nm. The fluorescence signals are shown at the bottom of the figure. Curve a shows most of the beam Doppler profile, the saturation dip and the narrow Ramsey fringes. Curves b-d show the fluorescence signals obtained near resonance for two separated laser beams (b), for three beams (c), and for four beams (d), respectively (the distance between first and last zones is the same for c and d). (From reference[15].)

opposition of two cat's-eye retroreflectors to produce the parallel radiation zones intrinsically provides a stable spatial phase relationship from beam to beam [15]. Several fluorescent profiles are included in Figure 1. Curve (a) shows most of the

beam Doppler profile, the saturated absorption dip, and the fringes due to the atom's interaction with three equally spaced standing-wave radiation zones. Curve (b) is the fluorescence profile produced when the Ne beam interacts with only two standing waves. Consistent with our discussion earlier, the optical Ramsey fringes are averaged to zero. The spectral profiles of curves (c) and (d) show the interference fringes obtained when the atomic beam interacts with three and four equally spaced standing waves, respectively. Spectral line narrowing with little loss in signal (compared to the Lamb dip) is apparent. To a good approximation [13], the fringe pattern for equal relaxation constants γ is an exponentially damped cosine proportional to

$$(1/v^2) \exp[-(\omega - \omega'_0)^2 (w_0/v_r)^2] \cos[(\omega - \omega'_0)(2v_x L/w_0^2 - \gamma)(w_0/v_r)^2], \quad (13.8)$$

where $v^2 = v_r^2 + v_z^2$, $v_r^2 = v_x^2 + v_y^2$, $\omega'_0 = \omega_0(1 - v^2/2c^2 \pm \hbar k/2mc)$ and where c is the speed of light and $2\pi\hbar$ is Planck's constant. The shift in the natural resonance frequency due to photon recoil $\pm \hbar k/2mc$ and due to the second-order Doppler shift $v^2/2c^2$ has been explicitly included in the expression for ω'_0 . Usually, these terms are ignored but with long-lived transitions that afford higher resolution, subtle shifts and distortions of the saturated absorption resonance caused by these terms can be seen. Conservation of 4-momentum (momentum and energy) requires that, in absorption, the atom absorb the energy and momentum of the photon, thereby changing not only the atom's internal energy, but also its motional energy. Similarly, in the emission process the atom must change its kinetic and internal energy to provide for the emitted photon's energy and momentum. Thus, the frequency of the absorbed photon is blue-shifted relative to the Doppler-shifted natural resonance frequency of the atom and, correspondingly, the emitted photon is red-shifted. In linear spectroscopy, the frequency shift due to the photon recoil cannot be directly detected, but in saturation spectroscopy, photon recoil manifests itself as a spectral doublet. There are two frequencies of anomalously high transmission for the probe wave. One occurs at the frequency where the atom's ground state density is reduced by the power wave interacting with the same set of absorbers. The second transmission peak comes at the frequency where the power wave interacts with the same velocity class of excited-state absorbers. The two peaks are symmetrically displaced about the Bohr frequency, with a frequency splitting $\delta\omega = \hbar k^2/m$. Early high-resolution experiments in saturation spectroscopy [18–21] fully resolved the recoil doublet and demonstrated the possibility of a direct frequency measurement of \hbar/m for atomic systems. Laser-cooling has renewed interest in the precise measurement of atomic recoil (better described now in terms of optical atomic interferometers with single-photon or two-photon beamsplitters [22]) both for an alternative determination of the fine structure constant through $\alpha^2 = (2R_\infty/c)(\hbar/m)(m/m_e)$ [23] and for a new mass standard [24] (R_∞ is the Rydberg and m_e is the mass of the electron).

The line center and spectral shape become highly sensitive to resolving power when the fractional frequency of resolution approaches that of the second-order Doppler shift [19, 25, 26]. This is particularly true for Ramsey spectroscopy with thermal beams. The resonance frequency for a particular velocity v is shifted by $-(v/c)^2/2$, but the interfringe spacing is proportional to $v/2L$ (assuming $v_x \approx v$). Velocity averaging washes out the fringe structure away from the spectral line center, because each cosine, with period dependent on v , contributes coherently only at line center, but adds with random phase elsewhere. When the interference fringe spacing begins to approach the same order of magnitude as the second-order Doppler shift, then there is no frequency, or "line center," where all velocity contributions add coherently. Rather, there is an arbitrary frequency position which receives the greatest portion of constructive interference that depends on the interzone spacing and on the atomic beam velocity distribution. Experiments in which a thermal beam of calcium ions was probed by the saturated absorption Ramsey method using widely separated beams revealed lineshapes that were distorted by second-order Doppler effects [19, 25]. But recent, beautiful work with cold atoms and Ramsey interrogation with pulsed beams has virtually eliminated problems due to second-order Doppler shifts [27].

13.5 Two-Photon Spectroscopy

Doppler-free two-photon spectroscopy is not as hampered by transit-time effects as linear- and saturated-absorption spectroscopy. If two photons of the same energy are absorbed from counter-running beams whose wavevectors are strictly opposed, then there is no momentum transfer between the electromagnetic field and the atom, and consequently no Doppler broadening, independent of the particles' motion. Long interaction regions are possible with simple optics and reasonably collimated atomic beams. Power broadening and shift and second-order Doppler effects tend to be the obstructions to higher resolution in two-photon experiments. The most familiar source of power broadening is saturation, which occurs whenever the incident laser intensities are sufficiently strong to equalize the populations of the two states connected by the nonlinear transition. This effect only broadens the lineshapes. There will also be a second-order shift between any pair of energy levels connected by an electric dipole interaction with an square of the oscillating electric field. In general, the light shift (AC Stark shift) is proportional to the square of the on-resonance Rabi rate divided by the detuning, $(\boldsymbol{\mu} \cdot \mathbf{E}/\hbar)^2/(\omega - \omega_0)$ [3, 4], where $\boldsymbol{\mu}$ is the atomic dipole moment and \mathbf{E} is the amplitude of the field. In linear or saturation spectroscopy, the light shift goes unnoticed because the atomic transition frequency is moved symmetrically about the line center. For red detuning, the

coupled energy states are pushed apart; for blue detuning, the levels are pushed together. The magnitude of the light shift is the same but oppositely directed for equal detunings away from resonance. Hence, the observed spectral feature is unshifted. Unfortunately, light shifts can never be entirely eliminated in two-photon spectroscopy, because the transition between levels is made by virtual, dipole-allowed transitions through intermediate states that are usually far from resonance. To find the quadratic frequency shift of either atomic level connected by the two-photon transition, it is necessary to sum over all intermediate states [3, 4]:

$$\Delta w_i = (1/4\hbar^2) \sum \{ |\boldsymbol{\mu}_{ni} \cdot \mathbf{E}|^2 / (\omega_{ni} - \omega) + |\boldsymbol{\mu}_{ni} \cdot \mathbf{E}|^2 / (\omega_{ni} + \omega) \}. \quad (13.9)$$

The difference of the individual shifts to the initial and final states makes up the optical Stark shift for the two-photon transition. Equation (13.9) shows that the effect is proportional to intensity, while the two-photon absorption signal is proportional to the square of the intensity. The persistence of a light shift in two-photon spectroscopy for arbitrary light intensities makes difficult the precise determination of the unperturbed line center. Nonuniform field intensities and different atom-field interaction histories further complicate the spectral shape. Experiments done at several intensity levels help extrapolate the Stark shift to zero intensity, but often brute-force computer analysis is needed to decipher the unshifted position of the line center [28].

One proposal to reduce the quadratic shift and at the same time preserve the signal strength was to use the Ramsey method of separate interrogation regions, whereby the atom spends most of its time freely precessing between sequential interactions with the high-intensity field(s). It was expected that the Stark shift would be diluted by the ratio of the dark-precession time to the field-interaction time. But, while this effect was seen in the shift of the line-center position of the Ramsey signal relative to that of the two-photon signal from a single interaction region [26], properly the comparison should be made between a Ramsey two-photon signal and a single-zone two-photon signal that are of equal amplitude *and* resolution. Because the probability of two-photon excitation depends on the product of the interaction time and the square of the field intensity, the single-zone intensity can be proportionately lowered if the interaction time is increased. Hence, no difference is expected in the magnitude of the Stark shift if the resolution and probability for excitation remain the same. Unfortunately, Doppler-free two-photon spectroscopy is never free of AC Stark effects.

Second-order Doppler effects also persist for moving atoms in two-photon spectroscopy. The spectral line shape is largely unaffected if the effective line width is much larger than the second-order shift $\omega_0(v/c)^2$. The shift remains, but it is probably not important in this case. When the spectral resolution is increased until it is comparable to or exceeds the second-order shift for the mean thermal velocity, then the line shape is also distorted. For a Maxwell-Boltzmann velocity

distribution, Minogin [29] finds a sharply asymmetrical line profile whose peak height is red-shifted by $(\omega_0/2)(u/c)^2$ (the line center is difficult to define).

The first demonstrations of Doppler-free two-photon absorption were done by several groups using atomic sodium [1, 3, 4]. Since then, two-photon spectroscopy has been used to study a great many transitions between states of the same parity and to determine term values, pressure shifts, broadening coefficients, and other parameters. Without question, however, the example for two-photon spectroscopy that is rich in physics and storybook in character is the continuously increasing precision spectroscopy of hydrogen that has been orchestrated by Professor Hänsch over the past two decades. Spectral studies of hydrogen have already played an important role in the development of atomic physics and quantum mechanics, from the Balmer spectrum and the Bohr model to the Lamb shift and QED. Largely because of its simplicity, it remains a dominant tool in Hänsch's research. Much of his work centers around the narrow two-photon transition from the $1S$ ground state to the metastable $2S$ state ($\gamma_{2s} \approx 7$ Hz). A direct frequency measurement of this transition has produced the most accurate measurement of the Rydberg constant [30]. The frequency difference between the $1S$ - $2S$ two-photon transition in hydrogen and in deuterium has provided a precise measure of the RMS structure radius of the deuteron [31]. In addition, the direct frequency comparison of the $1S$ - $2S$ transition to the $2S$ - $4S$ two-photon transition has furnished a measurement of the ground state Lamb shift to an accuracy of 6 ppm [32], which exceeds the best RF measurements of the $2S$ Lamb shift. Better precision is still expected. Figure 2 [33] shows spectra of the $F = 1$ hyperfine component of the hydrogen $1S$ - $2S$ two-photon transition at different nozzle temperatures. The asymmetry and shift due to the second-order Doppler effect are readily apparent. Cooling the atoms to a temperature near 8.6 K brings a fractional resolution of 1×10^{-11} (presently limited by laser frequency fluctuations). An enjoyable summation of these results and future possibilities can be found in reference [33].

13.6 Trapped Particle Spectroscopy at the Dicke Limit

Doppler-free spectroscopy is possible if the spatial excursions of an atom are constrained to less than the wavelength λ of the transition probed [10]. In the RF and microwave region, this condition, referred to as the Lamb-Dicke criterion, is easily satisfied because the radiation wavelengths are several centimeters and longer. At shorter wavelengths, tightly confining particles generally introduces other perturbations which are detrimental to line narrowing. Ion traps, in which ions undergo approximately simple harmonic motion, constrain particles virtually without perturbation [34]. In the optical region, the Dicke criterion was finally satisfied for a single, laser-cooled ion tightly, but benignly, confined in a

miniature RF Paul trap [35, 36]. (Coulomb repulsion between ions makes it difficult, but not impossible, to meet the Lamb–Dicke criterion when more than one ion is in the trap [37].) Spectral narrowing by this method can be understood by transforming the electric field vector into the rest frame of the atom

$$\mathbf{E}(\mathbf{r}(t), t) = \mathbf{E}_0 \cos(\omega t + \mathbf{k} \cdot \mathbf{r}(t) + \phi). \quad (13.10)$$

Recall that $|\mathbf{k}| = 2\pi/\lambda$. If $|\mathbf{r}(t)| \ll \lambda$, then $\mathbf{k} \cdot \mathbf{r}(t) \rightarrow 0$ independent of the relative direction of motion. The atom begins to accumulate (lose) phase during the first half of its cycle, but before gaining (losing) π radians and losing coherence with the field, it reverses its direction and returns to the original phase setting. Hence, the only significant response of the atomic system occurs at $\omega = \omega_0$.

The second-order Doppler shift of an ion that is laser-cooled to about 1 mK (which is near the Doppler-cooling limit for most ions using a strongly allowed transition) is around one part in 10^{18} . It also appears that, for a single ion shifts of resonance frequencies owing to electric and magnetic fields could be as small as one part in 10^{18} , since the ion is trapped in a region where the electric field approaches zero. Signal-to-noise ratio suffers when the sample under observation consists of only a single ion, or at most a few. However, once an ion has been trapped and cooled, its presence can be detected easily by laser-induced fluorescence, since a strongly allowed transition can scatter as many as 10^8 photons per

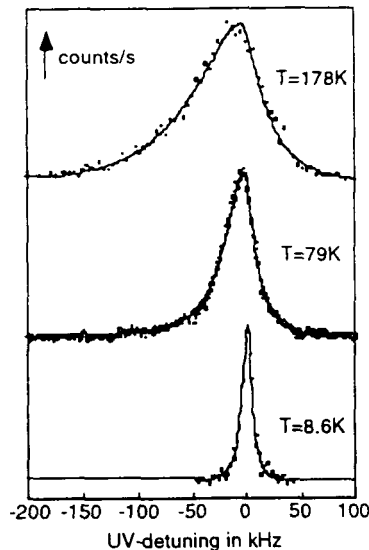


Fig. 2. Doppler-free two-photon spectra of the hydrogen $1S-2S$ transition observed in an atomic beam. The $F = 1$ hyperfine component has been recorded at different nozzle temperatures. The asymmetry and shift caused by second-order Doppler effects are greatly reduced at $T = 8.6$ K. (From reference [33].)

second. More importantly, a transition with a narrow natural linewidth can be detected with nearly unit efficiency by the presence or absence of the strong fluorescence [39]. Consider an atom that has both a strongly allowed transition and a weakly allowed transition that share the ground state. Then the narrow transition is detected as follows: The atom is assumed to be initially in the ground state. Radiation at a frequency near the weak resonance is pulsed on, possibly causing a transition to the long-lived upper level. Next, light with a frequency near that of the strong transition is pulsed on. If the atom had made a transition in the previous step, no fluorescence will be observed; otherwise, fluorescence will be observed at an easily detectable level. The detection of the presence or absence of fluorescence from the strongly allowed transition is much easier than attempting to detect the one photon that eventually is emitted when the metastable state decays. Detecting each transition to the metastable state makes it possible to achieve a signal-to-noise ratio that is limited only by the quantum statistical fluctuations in making the weak transition [36, 38].

Figure 3 [36] shows the fully resolved recoilless optical resonance and motional sidebands of the narrow S - D transition at $\lambda = 282$ nm on a single, laser-cooled $^{198}\text{Hg}^+$ ion confined in a miniature RF Paul trap. Each *single-photon* transition to the electric-quadrupole-allowed metastable D state ($\tau > 0.1$ s) was

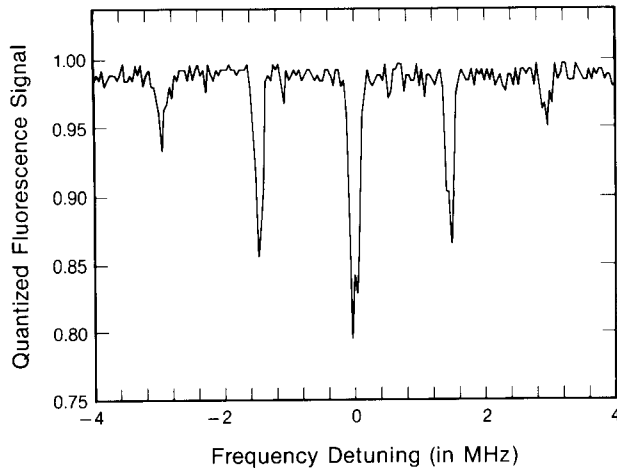


FIG. 3. Quantized signal showing the electric-quadrupole-allowed S - D transition ($\lambda = 282$ nm) in a single, laser-cooled $^{198}\text{Hg}^+$ ion. On the vertical axis is plotted the probability measure of observing fluorescence from the S - P first resonance transition at 194 nm as a function of the relative detuning of the 282-nm laser from line center. The S - D transition and the S - P transition are probed sequentially to avoid light shifts and broadening on the narrow S - D transition. The integration time per point is about 16 s. Clearly resolved are the Doppler-free absorption resonance and the Doppler sidebands due to residual secular motion of the laser-cooled ion. (From reference [36].)

detected with nearly unit efficiency by monitoring for the presence (no transition made) or absence (weak transition made) of fluorescence from the strongly allowed S - P transition at 194 nm. Note the absence of background or any instrumental noise. The fractional resolution of this spectrum already exceeded 3×10^{-11} .

More recently [40], the spectral linewidth observed for this transition, limited by the frequency fluctuations in the probe laser, was less than 80 Hz, corresponding to a fractional resolution of less than 1×10^{-13} . Laser cooling to the zero-point energy of the trap's harmonic well has reduced the spatial excursions of a trapped ion to less than 2.5 nm [41]. Very recently, laser-cooled neutral atoms have also been confined to the Lamb-Dicke regime in optical wells generated by crossed laser beams [42, 43]. However, neutral trapping can only be done by exchange of internal and kinetic energy; therefore, by its nature, it must perturb the internal energy level structure of the atom.

Trapped ions that are laser-cooled to the Doppler-cooling limit (which may not produce a spatial confinement less than an optical wavelength) offer perhaps the highest potential for spectral resolution and accuracy. Atom-field interaction times can be arbitrarily long (days), which not only eliminates interaction-time broadening, but also makes it possible to saturate weakly allowed transitions. For example, the electric-quadrupole-allowed, S - D transition in mercury can be saturated with as few as 10 photons per second focused to about λ^2 , if the laser line width is less than the natural linewidth. (This transition is also two-photon allowed, but remember that two-photon spectroscopy is burdened by light shifts.) Doppler effects are eliminated, or greatly reduced, to all orders. Perturbations due to collisions, already extremely small in room-temperature traps at pressures below 10^{-8} Pa (10^{-10} torr), can be virtually eliminated in a cryogenic environment. There are no first-order electric field shifts, and higher-order electric field shifts, as well as magnetic field shifts, can be reduced to below one part in 10^{18} . Two-photon spectroscopy can complement linear spectroscopy of trapped ions to reach states of like parity, which may be difficult, if not impossible, to reach otherwise. If the ions are cooled nearly into the Lamb-Dicke regime, the two-photon resonance will be Doppler-free independent of the light-beam directions (note that only a single beam is now necessary!). Prospects for all the methods seem exciting.

References

1. Shimoda, K., ed. (1976). *High-Resolution Laser Spectroscopy*. Springer-Verlag, Berlin.
2. Ramsey, N. F. (1956). *Molecular Beams*. Oxford University Press, London.
3. Letokhov, V. S., and Chebotayev, V. P. (1977). *Nonlinear Laser Spectroscopy*. Springer-Verlag, Berlin.

4. Levenson, M. D. (1982). *Introduction to Nonlinear Laser Spectroscopy*. Academic Press, New York.
5. Bennet, W. R., Jr. (1962). *Phys. Rev.* **126**, 580.
6. Lee, P. H., and Skolnick, M. L. (1967). *Appl. Phys. Lett.* **10**, 303.
7. Hänsch, T. W., and Toschek, P. (1968). *IEEE J. Quant. Electron.* **QE-4**, 467.
8. Vasilenko, L. S., Chebotayev, V. P., and Shishaev, A. V. (1970). *JETP Lett.* **12**, 113.
9. Cagnac, B., Grynberg, G., and Braben, F. (1974). *Phys. Rev. Lett.* **32**, 643; Levenson, M. D., and Bloembergen, N. (1974). *Phys. Rev. Lett.* **32**, 645.
10. Dicke, R. H. (1953). *Phys. Rev.* **89**, 472.
11. Hänsch, T. W., and Schawlow, A. L. (1975). *Opt. Commun.* **13**, 68.
12. Wineland, D. J., and Dehmelt, H. (1975). *Bull. Am. Phys. Soc.* **20**, 637.
13. Ramsey, N. F. (1950). *Phys. Rev.* **78**, 695.
14. Baklanov, Ye. V., Dubetsky, and Chebotayev, V. P. (1976). *Appl. Phys.* **9**, 171.
15. Bergquist, J. C., Lee, S. A., and Hall, J. L. (1977). *Phys. Rev. Lett.* **38**, 159.
16. Bordé, Ch. J., Salomon, Ch., Avrillier, S., van Lerberghe, A., Bréant, Ch., Bassi, D., and Scoles, G. (1984). *Phys. Rev. A* **30**, 1836.
17. Helmcke, J., Zevgolis, D., and Yen, B. U. (1982). *Appl. Phys. B* **28**, 83.
18. Hall, J. L., Bordé, Ch. J., and Uehara, K. (1976). *Phys. Rev. Lett.* **37**, 1339.
19. Bergquist, J. C., Barger, R. L., and Glaze, D. J. (1979). In *Laser Spectroscopy IV*, H. Walther and K. V. Rothe (eds.), p. 120. Springer-Verlag, Berlin.
20. Barger, R. L., Bergquist, J. C., English, J. C., and Glaze, D. J. (1979). *Appl. Phys. Lett.* **34**, 850.
21. Helmcke, J., Ishikawa, J., and Riehle, F. (1989). In *Frequency Standards and Metrology*, A. De Marchi (ed.), p. 270. Springer-Verlag, Berlin.
22. Borde, Ch. J. (1989). *Physics Letters A* **140**, 10.
23. Weiss, D., Young, B., and Chu, S. (1993). *Phys. Rev. Lett.* **70**, 2706.
24. Wignall, J. W. S. (1992). *Phys. Rev. Lett.* **68**, 5.
25. Barger, R. L. (1981). *Opt. Lett.* **6**, 145.
26. Lee, S. A., Helmcke, J., and Hall, J. L. (1979). In *Laser Spectroscopy IV*, H. Walther and K. V. Rothe (eds.), p. 130. Springer-Verlag, Berlin.
27. Sengstock, K., Sterr, U., Hennig, G., Bettermann, D., Müller, H. and Ertmer, W. (1993). *Opt. Commun.* **103**, 73 (1993).
28. Biraben, F., Garreau, J. G., Julien, L. and Allegrini, M. (1989). *Phys. Rev. Lett.* **62**, 621.
29. Minogin, V. G. (1976). *Kvantovaya Elektronika* **3**, 2061.
30. Andrae, T., König, W., Wynands, R., Leibfried, D., Schmidt-Kaler, F., Zimmermann, C., Meschede, D., and Hänsch, T. W. (1992). *Phys. Rev. Lett.* **69**, 1923.
31. Schmidt-Kaler, F., Liebfried, D., Weitz, M., and Hänsch, T. W. (1993). *Phys. Rev. Lett.* **70**, 2261.
32. Weitz, M., Huber, A., Schmidt-Kaler, F., Liebfried, D., and Hänsch, T. W. (1994). *Phys. Rev. Lett.* **72**, 328.
33. Hänsch, T. W. (1994). In *Atomic Physics 14*, D. J. Wineland, C. E. Weiman, and S. J. Smith (eds.), p. 63. American Institute of Physics, New York.
34. Dehmelt, H. S. (1967). *Advan. Atomic and Mol. Physics* **3**, 53; (1969). *Advan. Atomic and Mol. Physics* **5**, 109.
35. Janik, G., Nagourney, W. and Dehmelt, H. (1985). *J. Opt. Soc. Am. B* **2**, 1251.
36. Bergquist, J. C., Itano, W. M., and Wineland, D. J. (1987). *Phys. Rev. A* **36**, 428.
37. Raizen, M. G., Gilligan, J. M., Bergquist, J. C., Itano, W. M., and Wineland, D. J. (1992). *Phys. Rev. A* **45**, 6493.

38. Wineland, D. J. (1984). *Science* **226**, 395.
39. Dehmelt, H. G. (1975). *Bull. Am. Phys. Soc.* **20**, 60.
40. Bergquist, J. C., Itano, W. M., and Wineland, D. J. (1994). In *Frontiers in Laser Spectroscopy*, T. W. Hänsch and M. Inguscio (eds.), p. 359. North Holland, Amsterdam.
41. Diedrich, F., Bergquist, J. C., Itano, W. M., and Wineland, D. J. (1989). *Phys. Rev. Lett.* **62**, 403.
42. Jessen, P., Serz, C., Lett, P., Phillips, W., Rolston, S., Spreuw, R., and Westbrook, C. (1992). *Phys. Rev. Lett.* **68**, 3861.
43. Phillips, W. D. (1995). In *Atomic Physics 14*, D. J. Wineland, C. E. Weiman, and S. J. Smith (eds.), p. 211 and references therein. American Institute of Physics, New York.